Int. J. Electrochem. Sci., 10 **(2015)** 10726 - 10737

International Journal of
ELECTROCHEMICAL
SCIENCE
www.electrochemsci.org

The Impact of Ultraviolet Illumination on the Initial Atmospheric Corrosion of the Copper Covered by $(NH_4)_2SO_4$ Thin Electrolyte Layer

Qing Li Cheng[1,2,*], *Bin Tao*[1], *Wei Hua Zhang*[1], *Shuan Liu*[3], *Baorong Hou*[4]

[1]SINOPEC Qingdao Research Institute of Safety Engineering, NO.218, Yanan 3th Road, Qingdao 266700, Shandong province, P. R. China
[2]SINOPEC Research Institute of Petroleum Processing, 18, Xueyuan Road, Haidian District, Beijing, P. R. China.
[3]Institute of Materials Technology, Ningbo Institute of Industrial Technology, Chinese Academy of Sciences, No.1219 Zhongguan West Road Zhenhai District Ningbo City Zhejiang Province 315201, P. R. China.
[4]National Engineering Research Center for Marine Corrosion Protection, Institute of Oceanology, Chinese Academy of Sciences, Qingdao 266071, Shandong province, China.
[*]E-mail: cql328@126.com

Received: 12 September 2015 / *Accepted:* 13 October 2015 / *Published:* 4 November 2015

This research analyzed the impact of ultraviolet illumination on the initial atmospheric corrosion of the copper using a thin electrolyte layer containing $(NH_4)_2SO_4$ through X-ray diffraction (XRD), electrochemical impedance spectroscopy (EIS), coulometric reduction techniques (CRT) and Mott–Schottky analysis. Results indicated ultraviolet (UV) illumination could more promote the formation of total corrosion products in comparison with Cu exposed in dark. UV illumination slightly influenced the formation of cupric corrosion product except for accelerating formation of cuprite (Cu_2O). The formation of n-type Cu_2O has been proved by Mott–Schottky analysis.

Keywords: Copper; Atmospheric corrosion; Electrochemical impedance spectroscopy; XRD; Ultraviolet illumination.

1. INTRODUCTION

$(NH_4)_2SO_4$ is taken as one of the main components of fine dust particles in the atmosphere, and is able to generate patinas which have same characteristics as that of natural patina in laboratory. The most plenty of ions shown in fine particles in urban atmosphere, include SO_4^{2-} and NH_4^+ with a ratio typically ranging between that of $(NH_4)_2SO_4$ and NH_4HSO_4. Previous studies have explored the effect

of submicron $(NH_4)_2SO_4$ particles on copper corrosion with different temperatures and relative humidities (RHs)[1-3]. The simulations in laboratory indicated that the particles of $(NH_4)_2SO_4$ result in the natural patinas' corrosion products. Principal components of patina have attracted lots of attentions for a long time. Cuprite (Cu_2O) is considered as the most common corrosion product being found in copper patinas . Other constituents can be present also by considering environmental feature. Copper hydroxysulfates, mainly brochantite ($Cu_4SO_4(OH)_6$) and antlerite ($Cu_3SO_4(OH)_4$) [4-6] are regarded as most common ingredients both in urban and industrial atmospheres.

At present, many research attentions have been paid to the impact of UV light in solar radiation on steels corrosion [7-9]. In fact, UV radiation not also affects steels: the results of Polarisation test showed that UV radiation is able to inhibit generation rate of pitting [10] and strengthen the passivity of SS304 in chloride solution [11,12]. In contrast, UV radiation also indicated apparent corrosion rate [13]. The weight loss of copper and zinc which were immersed in fresh water was shown to be greater in UV light than that in the dark [9]. However, negative influence of UV radiation on the passivity of zinc alloys' passivity was investigated [14]. Although UV illumination canpromote Cu sulfidation in the presence of H_2S [15], little research has been made on the impact of UV illumination on atmospheric corrosion of Cu with ammonium ion. The n-type Cu_2O formed in a slightly alkaline solution or acidic with pH 4 to 8 was found. The passive films genereated on the metal and alloys are shown to have semiconductor properties. Hence, transport rate of electron and ion in the film semiconducting properties of oxide mainly affect the corrosion rate upon. The measurement of anodic photocurrent and application of UV illumination were both carried out [16, 17]. Studying atmospheric corrosion of Cu under the effects of UV illumination is necessary.

The objective of this paper was UV illumination's influence on the Cu corrosion in an atmospheric environment. To illustrate the photo-induced atmospheric corrosion of Cu, relative experiments were performed by EIS and CRT.

2. EXPERIMENT

2.1 Materials

A pure Cu rod (>99.9 wt%,) with a diameter of 4 mm was applied in the experimental tests. The working electrode selected was conducted mechanical cutting from the pure Cu rod and introduced into the epoxy. This electrode system was ground to #3000 SiC paper before electrochemical tests, and then, a diamond paste of 2 μm performed fine polishing. Afterwards, this experiment washed the surface using the water distilled, by degreasing it with the acetone, the surface was dried by a cool air flow. In this experiment, the electrolyte was a $(NH_4)_2SO_4$ solution prepared by analytical grade reagent$(NH_4)_2SO_4$ and deionized water.

2.2 The experimental design

Fig. 1 shows the thin electrode layer (TEL) thickness (120 μm) determined [18]. The electrode was fixed in the cell with upper surface being merely exposed. To make thickness of electrolyte layer

being constant due to the evaporation of solution, a cell with a large area of 30 cm × 15 cm was employed. A 316 stainless steel wire with 1.5 mm in diameter was employed as the counter electrode by fixing it at the place surrounding the electrode and its positioned was below the surface exposed. Saturated KCl solution containing Ag/AgCl, as the reference electrode, was added in the bulk solution. Then, we horizontally set the electrochemical cell in a chamber at constant temperature. Although the electrolyte layer of the working electrode was found to be ultra thin, the counter and reference electrodes were remaining soaked in the bulk electrolyte.

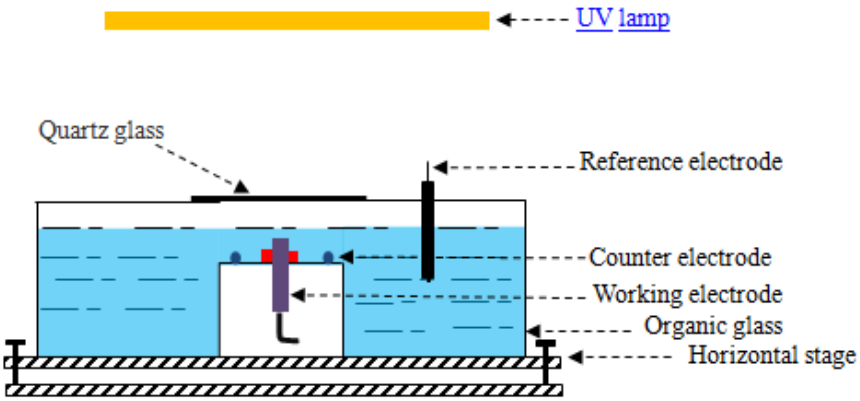

Figure 1. Schematic drawing of the electrochemical measurement in the TEL corrosion study with UV illumination.

UV light (254 nm) was sued as the illumination source. The top cover of this chamber was quartz glass window with 2 mm in thickness, which enabled UV light to passing through the chamber. While, the UV intensity at the top of the quartz window was set to 3.2 mW/cm^2. And then, the author exposed the Cu samples under UV illumination unless they were exposed in the dark..

2.3 Identifying and quantifying corrosion product

The products of corrosion were characterized using XRD. Then, the amount of corrosion products was quantified by CRT by applying 0.1 mol L^{-1} Na_2CO_3 as the supporting electrolyte[19]. Besides, reduction current density was set to a constant-0.2 mA cm^{-2} and a ordinary flat cell of three-electrode were employed to conduct reduction test. Moreover, the Ag/AgCl electrode comprising KCl solution saturated and a platinum sheet were used the reference electrode and an auxiliary electrode. Ag/AgCl electrode can be seen in all potentials discussed in this research.

2.4 Electrochemical measurements

The electrochemical measurement in this research was performed at the electrochemical workstation of CHI660D purchased from Shanghai Chenhua Device Co., Ltd, China. EIS was used to

carry out measurements by setting the frequencies ranging from 100 kHz to 10 mHz at open circuit potential while the potential perturbation is ±5 mV. EIS spectra for the electrode containing NaCl particles were conducted *in situ* measurement in the test atmospheric chamber.

Mott–Schottky (M–S) measurement was performed at 1 kHz frequency by scanning the potential from +0.5 V (vs. Ag/AgCl) to -0.5V (vs. Ag/AgCl) negative direction in 50 mV/min steps.

3. RESULTS AND DISCUSSION

3.1 EIS measurements

In this work, the atmospheric corrosion behaviors for Cu under TEL were analyzed under UV illumination and dark conditions respectively. EIS results obtained are illustrated in Figs. 2 and 3. As seen from Figs. 2b and 3b, three time constants are found.

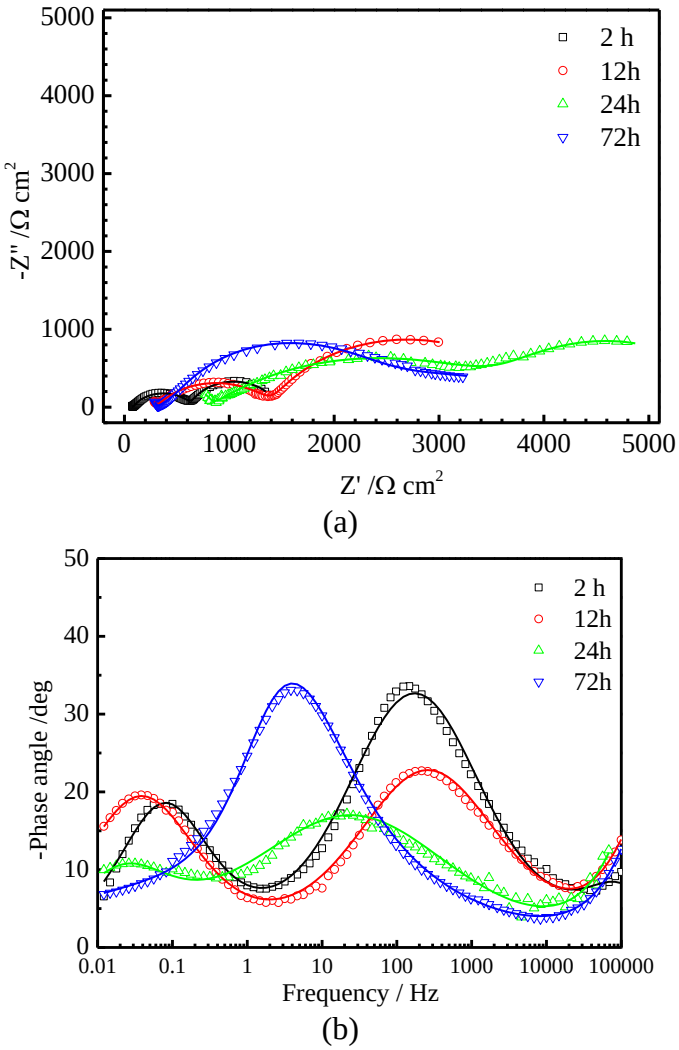

Figure 2. Experimental (dots with different symbols) and fitted (solid lines) impedance diagrams for copper under TEL with dark condition: (a) Nyquist plots and (b) Bode phase angle plots.

To fit the EIS curves as shown in Fig. 4, equivalent circuit of three time constants was utilized. R_s indicates the resistance of solution, C_o and R_o are the capacitance and resistance of oxide film respectively, CPE-*f* is a constant phase element ofto the film capacitance of corrosion products , R_f is the film resistance of the corrosion products, while CPE-dl is a constant phase element of double layer capacitance, R_{ct} is a resistance of charge transfer.

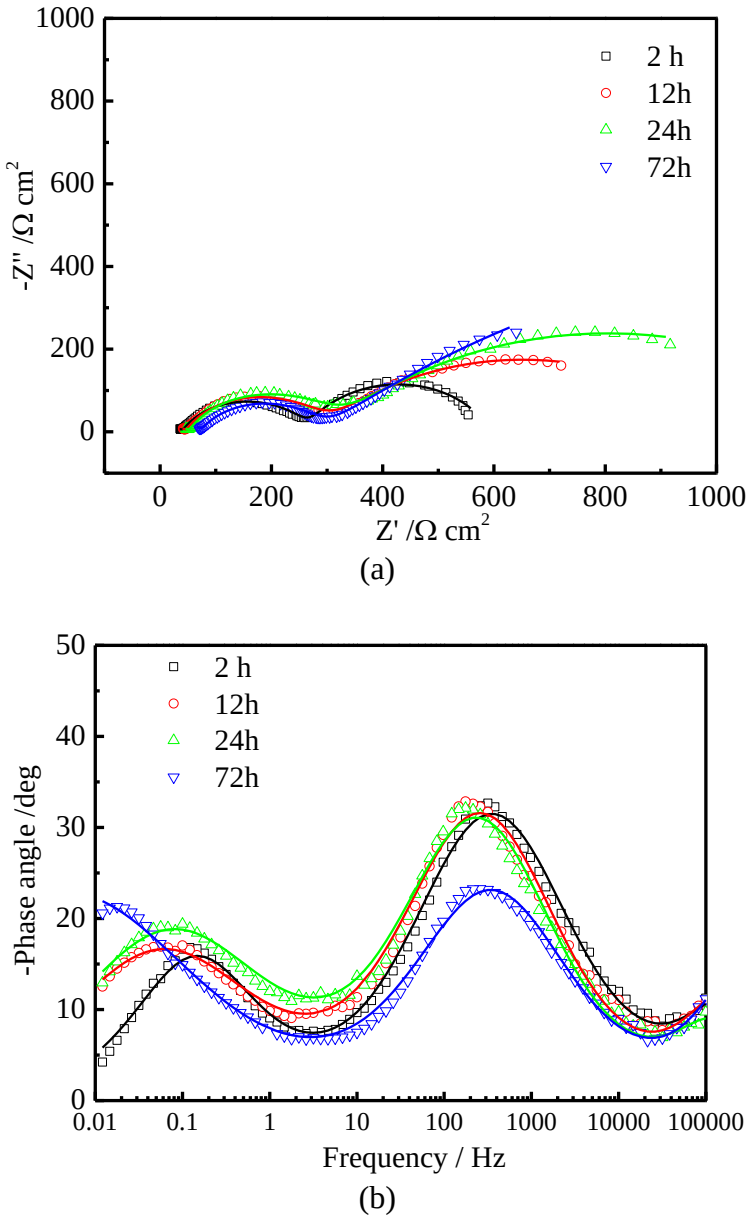

Figure 3. Experimental (dots with different symbols) and fitted (solid lines) impedance diagrams for copper under TEL with UV illumination: (a) Nyquist plots and (b) Bode phase angle plots.

Figs. 2 and 3 demonstrated that the given three equivalent circuits could well fit the experimental results in most of the frequency range. They therefore were shown to be suitable for interpreting the EIS data in the experiment.

Table 1. Fitted parameters of EIS measurements of copper covered by TEL with UV illumination and dark conditions during 72 h of exposure.

	Time (h)	R_s (Ω cm^2)	C_o ($nFcm^{-2}$)	R_O (Ω cm^2)	CPE-*f* (μFcm^{-2} Hz^{1-n_f})	n_f	R_f (Ω cm^2)	CPE-*dl* (μF cm^{-2} $Hz^{1-n_{dl}}$)	n_{dl}	R_{ct} (Ω cm^2)
Dark	2	64.6	91.3	20.8	35.8	0.70	566.3	3362	0.85	809.5
	12	137.8	3.9	171.1	17.0	0.64	1117	1882	0.75	2587
	24	323.8	1.5	482.9	63.6	0.48	3159	3008	0.82	1928
	72	80.5	2.0	217.3	704.3	0.35	2728	98.3	0.88	1424
UV	2	27.2	85.2	12.6	48.2	0.71	232	5037	0.78	321.2
	12	30.4	72.4	15.3	49.1	0.72	257.1	4634	0.58	707.3
	24	38.2	101.3	13.7	46.6	0.72	273	3168	0.57	974
	72	43.8	27.5	28.6	46.4	0.69	221.6	7225	0.49	2275

As shown in Table 1, the fitted parameters obtained using EIS for the copper exposed for 72 h on the conditions of UV illumination and darkness. Although R_p is often employed to indicate the corrosion rate [20], it has been proved to be significantly less accurate than R_{ct} in characterization of corrosion rate [21]. R_{ct} is merely obtained based on the faradic process of the corrosion controlled by charge transfer. The characterization corrosion rate using R_p showed a big error as R_p was acquired from the impedance diagram which had more than one time constant. R_{ct} values of UV illumination increased with exposure time revealed the decreased corrosion rate during the exposure of 72 h.

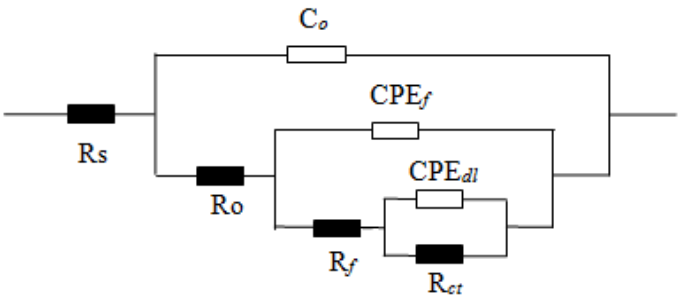

Figure 4. Equivalent circuits used for fitting the EIS data of copper covered by TEL with UV illumination and dark conditions during 72 h of exposure. R_s is the solution resistance, C_o is oxide film capacitance, R_o is oxide film resistance, CPE-*f* is a constant phase element corresponding to corrosion products film capacitance, R_f is corrosion products film resistance, CPE_{dl} is a constant phase element corresponding to double layer capacitance, R_{ct} is charge transfer resistance.

But R_{ct} values under dark condition experienced an increase firstly and then decreased in the exposure for 72.Through the comparison of R_{ct} values obtained under UV illumination and the dark, R_{ct} values obtained through UV illumination were smaller than that in the dark in first 24 h. This phenomenon showed that corrosion rate was improved by using UV illumination in first stage. However, there was not such improving effect in the later stage of 72 h. Meanwhile, Ta more protective layer on the copper, which is generated with the aid of UV showed inhibition effect. Therefore, the corrosion rate of UV illumination was found to be lower than that in the dark at 72 h.

3.2 Identification of corrosion products

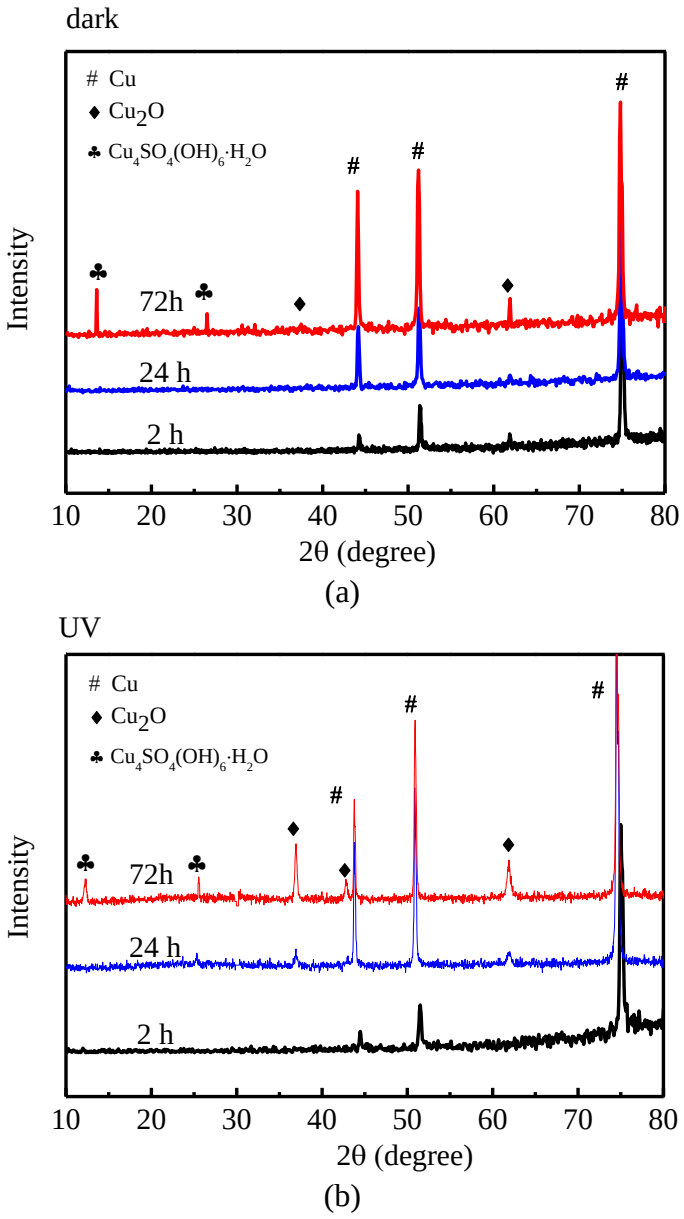

Figure 5. XRD spectra of the copper surfaces covered with TELs after exposure for 72 h (a) dark and (b) UV illumination.

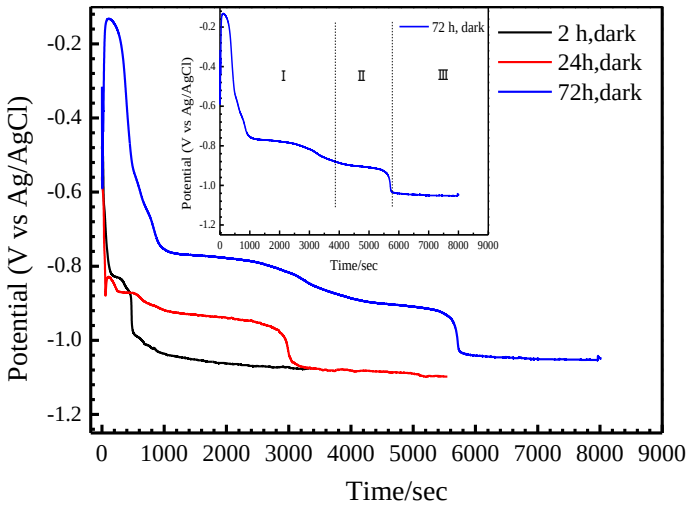

Figure 6. Reduction curve of the copper corrosion products exposed on dark condition under TEL: reduced in 0.1 mol L^{-1} Na_2CO_3 with −0.2 mA cm^{-2}.

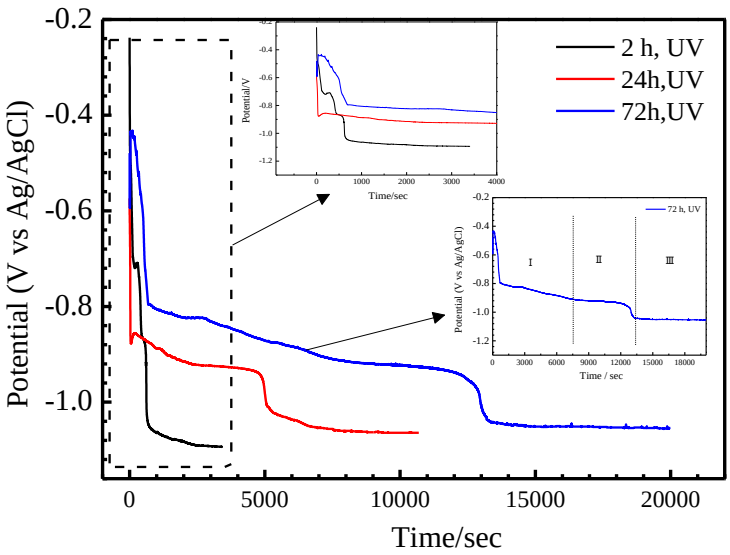

Figure 7. Reduction curve of copper corrosion products exposed under UV illumination under TEL: reduced in 0.1 mol L^{-1} Na_2CO_3 with −0.2 mA cm^{-2}.

Fig. 5 demonstrates the corrosion products of Cu which was exposed under UV illumination and the dark at varing times, respectively. After exposure for 72 h, the corrosion products were determined to be Cu_2O and cupric compounds using XRD. However no sufficient corrosion products were detected by XRD at the initial 2 h. As seen from Figs. 6 and 7, the reduction curves evidently show three intervals after exposure for 72 h: less than −0.91 V, the range from−0.91 to −1.0 V, and then hydrogen evolution at below −1.0 V. According to the previous study [22-25], the reduction potential of Cu_2O ranged from 0.75 to 0.9 V for saturated calomel electrode (SCE) in KCl, KOH or $Na_2B_4O_7$. In this study, compared with that on the SCE, the potential on the Ag/AgCl was lower (0.044 V). Hence the reduction of Cu_2O resulted in a reduction potential of -0.87 V (SCE) . Besides it also

exhibited a reduction plateau in which the potential was greater than −0.91 V (Ag/AgCl). This was owing to the reduction of cupric compounds even thougha cupric compound was not detected by XRD after the exposure for 2 h.

3.3 Quantification of corrosion products

The weight loss of Cu is determined based on the reduction curves as:

$$W = \frac{1000 \times (Q_c + 0.5 \times Q_p) \times M}{F} \quad (1)$$

where W represents total weight loss in g/m^2, Qc is the reduction charge indicating the Cu_2O reduction in C/cm^2, while Qp is a reduction charge referring to the reduction in cupric compounds in C/cm^2, while M indicates the molecular weight of Cu, 64 g/mol, and F is the Faraday constant for 96500 C/mol.

To calcualte total Cu weight loss, Qc and Qp are described in formulae. (2) and (3).

$$W_c = \frac{1000 \times Q_c \times M}{F} \quad (2)$$

$$W_p = \frac{1000 \times Q_p \times M}{2F} \quad (3)$$

Where W_c is the weight loss resulted from the Cu_2O formation, and W_p indicates the weight loss led by the cupric compounds formed in g/m^2. Though there were no cupric compounds being measured using XRD for the samples after exposure for 2 h, the charge for the reduction which was above the plateau of Cu_2O reduction was still able to be assigned to Q_p, because of the reduction of Cu^{2+} ions. Cu_2O was formed much faster than cupric compounds and its formation rate exerts the most apparent impact on the corrosion rate of Cu.

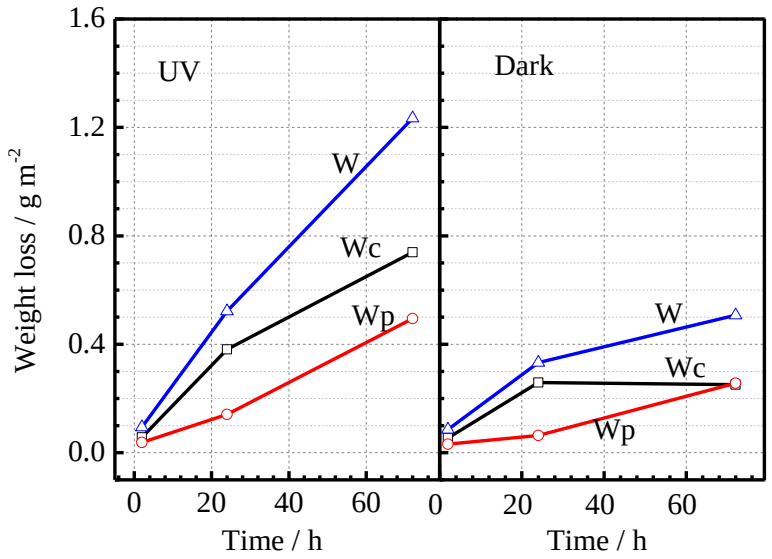

Figure 8. Weight loss and the loss in thickness of copper exposed on dark conditions and UV illumination. W is total weight loss in g/m^2, Wc is reduction charge corresponding to reduction of cuprite, Wp indicates reduction charge representing the reduction of cupric compounds.

As shown in Fig. 8, the weight losses of Cu with UV illumination and the dark at varying times are summarized. It reveals that because the formation rate of Cu_2O was increased by UV illumination in the exposure of 72 h, the addition of UV illumination improved the formation of total Cu corrosion products. Hence, the formation rate of cupric compounds with UV illumination merely showed a slighter increase than that in the dark. In general, the formation of Cu_2O on the Cu surface was shown to be the semiconductor with n-type [26] or p-type [27]. The p-type Cu_2O with a bandgap (2.4 eV) can generate cathodic photocurrent with UV illumination, which decreased passive current and rose corrosion rate. However, the p-type Cu_2O with a bandgap for 2 eV produced anodic photocurrent and improved the corrosion rate. Fig. 8 apparently demonstrates that accelerating effect of UV was possibly due to the formation of n-type Cu_2O.

3.4 Determination of n-type Cu_2O

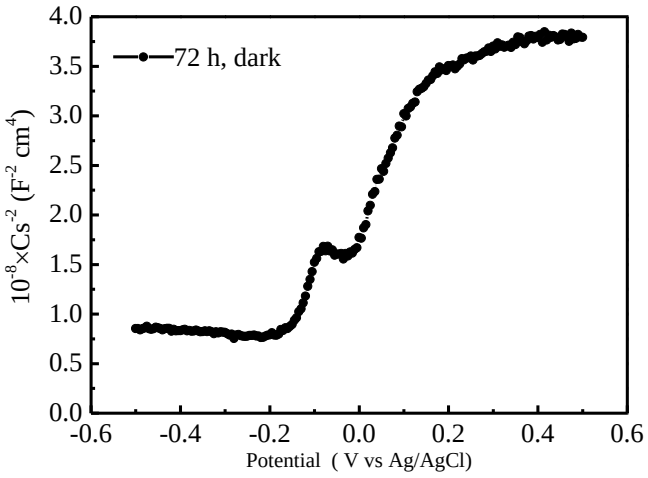

(a)

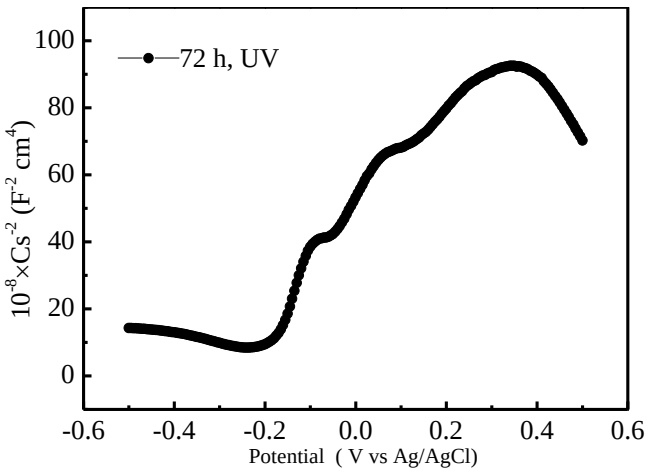

(b)

Figure 9. Curves of Mott–Schottky for copper exposed on (a) dark conditions and (b) UV illumination after exposure for 72 h.

The electric property of corrosion films is known to be studied by M–S[28] relation by measuring the electrode capacitance which serves as a function of the applied potential applied without concerning the capacitance on Helmholtz layer. M–S curve presented a positive slope for n-type semiconductor and showed a negative slope regarding p-type semiconductor. After being immersed for 72 h, the slope of the main straight-line portion of the characteristic M–S curve was found to be positive, even though the relating M–S plot in Fig. 9 comprised three stages.

This phenomenon distinctly verified that the corrosion product on the copper was n-type semiconductor Cu_2O in the case of a bandgap for 2 eV. N-type Cu_2O is able to cause anodic photocurrent and increase corrosion rate [19]. Fig. 8 indicates the apparent accelerating effect of UV. The n-type Cu_2O on the anodic area of Cu under UV illumination. A hole-electron pair tended to be formed as long as UV illumination with energy larger than bandgap struck n-type Cu_2O. The holes moved toward the surface; however the electrons were shown to migrate to the cathodic area under the effect of oxygen reduction. The research [19] put forward three possible pathways regarding formation of Cu_2O under UV illumination as the deposition rate of NaCl is constant. In our study, the photons may exert little influence on the formation of cupric ions. This could be validated by the minor increase of W_p under the illumination of UV compared to exposed Cu in the dark. Therefore, the UV illumination presented major effect on formation of Cu_2O.

4. CONCLUSIONS

The effect of UV illumination on the initial atmospheric corrosion of copper was studied under $(NH_4)_2SO_4$ thin electrolyte layer. The main conclusions can be drawn in the following:

1. The total weight loss of copper with UV illumination was more than that of dark
using EIS and coulometric reduction techniques.
2. XRD shows that the corrosion products ware Cu_2O and cupric compounds.
3. UV illumination accelerated formation of Cu_2O compared to Cu exposed in dark.
4. The acceleration effect of UV was attributed to the formation of n-type Cu_2O, which was verified by Mott–Schottky analysis.

ACKNOWLEDGEMENT
This work was financially supported by SINOPEC, We are grateful to professor Senior Engineer Xiaohui Liu to help.

References

1. R. E. Lobnig, C. A. Jankoski, *J. Electrochem. Soc.,* 145(1998) 946.
2. R. E. Lobnig, R. P. Frankenthal, D. Siconolfi, J. D. Sinclair, *J. Electrochem. Soc.,* 140(1993) 1902.
3. H. E. Lobnig, P. Frankenthal, D. J. Siconolfi, D. Sinclair, M. Stratmann, *J. Electrochem. Soc.,* 141(1994) 2935.
4. R. Holm, E. Mattsson, ASTM STP. 767, ASTM, Philadelphia (1982)

5. T.E. Graedel, K. Nassau, J.P. Franey, *Corros. Sci.*, 27(1987) 639.
6. I. Odnevall, C. Leygraf, *J. Electrochem. Soc.*, 142(1995) 3682.
7. P. Scmuki, H. Bohni, *Electrochim. Acta*, 40(1995) 775.
8. R. Wiesingera, M. Schreinera, Ch. Klebera, *Appl. Surf. Sci*., 256(2010) 2735.
9. T.D. Burleigh, C. Ruhe, J. Forsyth, *Corrosion (Houston, TX, U. S.).*, 59(2003) 774.
10. S. Fujimoto, T. Yamada and T. Shibata, *J. Electrochem. Soc.*, 145(1998) L79.
11. S. Moussa, M. Hocking, *Corros. Sci.*, 43(2001) 2037.
12. D. Macdonald, E. Sikora, M. Balmas, R. Alkire, *Corros. Sci.*, 38(1996) 97.
13. L. Rowe, *Corrosion*, 17(1997) 267t.
14. T. Burleigh, C. Ruhe, J. Forsyth, *Corrosion*, 59(2003) 774.
15. L. Volpe, P. Peterson, *Corros. Sci.*, 29(1989) 1179
16. F. Di Quarto, S. Piazza, and C. Sunseri, *Electrochim. Acta*, 30(1985) 315.
17. U. Bertocci, *J. Electrochem. Soc.*, 125(1978) 1598.
18. X. Liao, F. Cao, L. Zheng, W. Liu, A. Chen, J. Zhang, C. Cao, *Corros. Sci.* 53(2011) 3289.
19. H. Lin, G. S. Frankel, *J. Electrochem. Soc.*, 160(2013) C336.
20. A. Nishikata, Y. Ichihara, T. Tsuru, *Corros. Sci.*, 37(1995) 897.
21. Q.L. Cheng, Z.Y. Chen, *Int. J. Electrochem. Sc.*, 8(2013) 8282.
22. S. Nakayama, T. Kaji, M. Shibata, *J. Electrochem. Soc.*, 154(2007) C1.
23. J.Wang, F.L Cui, S.B Chu, X.Q Jin, J. Pu, Z.H Wang, *ChemPlusChem.*, 79(2014) 684
24. S. Swain, I. Thakur, S. Chatterjee, N.A. Kulkarni, P. Ayyub, Y.S. Chaudhary, *J. Appl. Phys.*, 117(2015) 303.
25. Y. Zeraatkish, M. Jafarian , F. Gobal, M. G. Mahjani, *J. Solid State Electrochem.*, 19 (2015) 2155.
26. M. Stratmann, H. Streckel, K.T. Kim, S. Crockett, *Corros. Sci.*, 30(1990) 715.
27. J.A. Calderon, C.E. Arroyave, *Corrosion*, 61(2005) 99.
28. F.P. Koffyberg, F.A. Benko, *J. Appl. Phys*., 53(1982) 1173.